



Reactivity of vanadium oxytrichloride with β -diketones and diesters as precursors for vanadium nitride and carbide



Ben J. Blackburn^a, Jared H. Crane^a, Caroline E. Knapp^a, Michael J. Powell^a, Peter Marchand^a, David Pugh^b, Joseph C. Bear^a, Ivan P. Parkin^a, Claire J. Carmalt^{a,*}

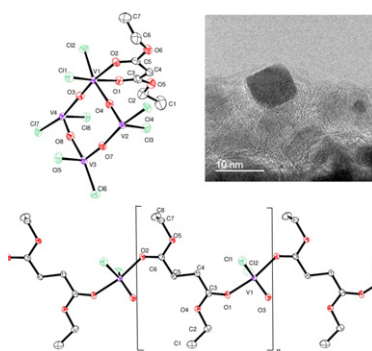
^a Materials Chemistry Centre, Department of Chemistry, University College London, 20 Gordon Street, London WC1H 0AJ, UK

^b Department of Chemistry, University of Southampton, Highfield, Southampton SO17 1BJ, UK

HIGHLIGHTS

- The synthesis of vanadium compounds Dichloro(oxo) (2,4-pentanedione) vanadium(V), Dichloro(oxo) (diethyl malonate) vanadium(IV) and Dichloro(oxo) (2,4-pentanedione) vanadium(V) are reported
- The compounds were evaluated as single source precursors for vanadium nitride and carbide.
- The synthesis of vanadium nitride or carbide could be effected by altering the gas under which these compounds were annealed at 1200 °C from nitrogen to argon.
- Dichloro(oxo) (diethyl malonate) vanadium(IV) produced phase pure vanadium nitride and carbide.

GRAPHICAL ABSTRACT



ARTICLE INFO

Article history:

Received 4 March 2016

Received in revised form 3 June 2016

Accepted 8 June 2016

Available online 16 June 2016

Keywords:

Vanadium oxychloride

Precursors

Ester adducts

Vanadium carbide

Vanadium nitride

Hard materials

ABSTRACT

Vanadium(V) oxytrichloride was reacted with 2,4-pentanedione, diethyl malonate, and diethyl succinate under inert conditions, forming compounds: dichloro(oxo)(2,4-pentanedione) vanadium(V) [1], dichloro(oxo)(diethyl malonate) vanadium(IV) [2] and dichloro(oxo)(diethyl succinate) vanadium(IV) [3]. Compounds 1–3 are coordinated to the vanadium centre through the two carbonyl oxygen atoms of the bidentate ligand. It was determined by X-ray crystallography that the structures of the resulting complexes were significantly different, resulting in a monomeric complex (1), a tetrameric ring (2) and a 1D coordination polymer (3). Following the synthesis and isolation of 1–3, they were tested as precursors for vanadium nitride and vanadium carbide by annealing under nitrogen and argon respectively at 1200 °C for 24 h. The resulting materials were characterised by: XRD, EDS, XPS and TEM.

© 2016 The Authors. Published by Elsevier Ltd. This is an open access article under the CC BY license (<http://creativecommons.org/licenses/by/4.0/>).

1. Introduction

Vanadium nitride (VN) and vanadium carbide (VC) are the subject of investigation for materials scientists due to their exceptional hardness, high melting points, high thermal conductivities and solid lubricating

* Corresponding author.

E-mail address: cj.carmalt@ucl.ac.uk (C.J. Carmalt).

properties [1–3]. The Vickers hardness of VC has been measured at 2600–3200 kg mm⁻² [4,5], considerably harder than tungsten carbide [6] and similar to titanium carbide (2400 kg mm⁻² & 1 1900–3200 kg mm⁻² respectively) [7] as well as a measured Young's modulus comparable with that of tungsten carbide [5,8,9]. VN exhibits similar properties, with a Vickers hardness of 1500 kg mm⁻² and high melting point (2619 K) comparable to VC (3103 K) [1,10].

VN is widely used to harden steel, with a layer of VN created on the surface of the steel by annealing at high temperatures under a flow of nitrogen. This increases wear resistance for use in high performance steels [11,12]. VN is also a strong coupled superconductor, with nanocrystalline VN having potential use in supercapacitors [13].

VN is often synthesised by controlled direct nitridation using nitrogen or ammonia gas at varying temperatures. In this way, foams of VN were formed through the nitridation of vanadium oxides with ammonia gas with high control over foam morphology [14]. Other methods include microwave synthesis [15–17], hydrothermal synthesis [18] and high temperature plasma routes [19].

VN thin films have been synthesised from molecular precursors such as NH(SiMe₃)₂ [20], VCl₄ [21,22] and V(NEt₂)₅ with a carrier gas composed of 10% NH₃ in He using atmospheric pressure chemical vapour deposition (APCVD) [23]. VN has also been produced from a variety of molecular precursors including: the direct reaction of vanadium tetrachloride with sodium amide [24], vanadium-urea complexes [25,26], chloroimidovanadium compounds and metal oxide nanoparticles with cyanamide and urea [27].

VC has been shown to be a highly effective additive to tungsten carbide in improving the hardness and thermal conductivity of highly durable ceramic-metal “cermet” composites [28], and an ideal material for improving the wear resistance of tools [29–33]. Furthermore precipitation of vanadium carbide nanoparticles into ferrite-martensite dual phase steel has been shown to cause a consistent improvement to Vickers hardness over a range of synthesis conditions [27–29]. It has been reported that depositing a layer of vanadium carbide onto the surface of high carbon steel *via* a salt bath has been shown to improve its surface hardness by six times [34]. A similar report detailed VC coatings deposited onto a die steel substrate *via* high temperature reactive diffusion using a NH₄Cl/ferro-vanadium/naphthalene precursor, resulting in surface hardness improved approximately fivefold [35].

Numerous methods for the formation of vanadium carbide nanoparticles exist in the literature. A family of preparations using vanadium(V) oxide (V₂O₅) with various carbonaceous species and reducing gaseous environments at high temperatures are widely used [28,36,37]. Refluxing V₂O₅ powder in *n*-dodecane has been shown to yield VC nanoparticles after several days [38], as has decomposition of V₂O₅ with magnesium filings and acetone in an autoclave [28,39–41]. Nanostructured thin films of vanadium carbide have been deposited using the chemical vapour deposition of single source molecular precursors such as: vanadocene [42], vanadocene dichloride and dimethyl vanadocene [43] and cyclopentadienyl vanadium tetracarbonyl [44].

We present a range of new molecular species derived from diester (2,4-pentanedione, diethyl malonate, and diethyl succinate) addition to VOCl₃ as single source precursors for vanadium nitride and carbide formation. The single source precursors presented herein are ideal for small scale laboratory preparations and applications of VN and VC, such as the synthesis of thin films, nanoparticles and nanofibres [45]. The chemistries and structures of the aforementioned molecular species were evaluated using X-ray crystallography (full structure determination and associated analysis), elemental analysis, ¹H and ¹³C {¹H} nuclear magnetic resonance (NMR) spectroscopy. Each of the precursors was converted to vanadium nitride and vanadium carbide *via* heating in furnace under an inert atmosphere at 1200 °C, similar temperatures to those used in the formation of austenitic steel [46,47]. The conversion to the carbide or nitride was dependent on the carrier gas used, with nitrogen giving the nitride and argon the carbide. This demonstrates the versatility of the single-source precursors presented herein over

multi-source methods, as by changing something as simple as the carrier gas, a completely different material is formed. It is also noteworthy that the vast majority of recent literature on the synthesis of both vanadium carbide and nitride focuses on the use of dual source precursors and complex formation *in situ* in the reaction vessel [48–53]. Reported scale-up and industrial scale processes use dual source routes, with vanadium pentoxide and carbon under different gaseous conditions for both vanadium carbide and nitride [54,55]. The use of single source precursors represents a significant step forward in precursor design for vanadium nitride and carbide, and offers potential advantages over dual source precursors for industrial scale-up as the amount of feedstocks would multiply, thus increasing costs. This route would also offer a more convenient synthetic method for lab-scale synthesis of both vanadium carbides and nitrides. The conversion to vanadium carbide and nitride was examined by X-ray diffraction (XRD), X-ray photoelectron spectroscopy (XPS), energy dispersive X-ray spectroscopy (EDS) and transmission electron microscopy (TEM).

2. Experimental

All starting materials were purchased from Sigma Aldrich and used without further purification. The solvents were dried over activated alumina by the Grubbs method using anhydrous engineering equipment, such that the water concentration was 5–10 ppm [56]. All products were synthesised under an atmosphere of nitrogen obtained from BOC in anhydrous solvents using standard Schlenk techniques. ¹H and ¹³C {¹H} NMR spectroscopy was carried out on a Bruker A-600 MHz spectrometer, operating at 295 K and 600.13 MHz (¹H). Signals are reported relative to SiMe₄ (δ = 0.00 ppm) and the following abbreviations are used s (singlet), d (doublet), t (triplet), q (quartet), m (multiplet), b (broad). Deuterated CDCl₃ was obtained from GOSS Scientific and was degassed and dried over 3 Å molecular sieves.

2.1. Synthesis of dichloro(oxo)(2,4-pentanedione) vanadium(V) [1]

2,4-Pentanedione (acacH) (0.5 cm³, 4.87 mmol) was added dropwise to VOCl₃ (2 cm³, 21.1 mmol) in 30 cm³ of *n*-hexane and stirred under nitrogen for 2 h. A dark precipitate formed immediately, giving a solution that appeared black. The precipitate was filtered and washed with *n*-hexane and dried *in vacuo*. This afforded the dark red complex **1** (1.1 g, 75%). Crystals suitable for single crystal X-ray diffraction were grown by layering a saturated solution of **1** in dichloromethane with hexane. Large green crystals formed over the course of 2 days. ¹H NMR (CDCl₃): δ 2.39 (s, 6H, CH₃), 6.13 (s, 1H, CH). ¹³C {¹H} NMR (CDCl₃): δ 26.4 (CH₃), 105 (CH), 193 (C=O). Elemental analysis calculated for VO₃Cl₂C₅H₇: C, 25.34; H, 2.98. Found: C, 25.80; H, 3.02.

2.2. Synthesis of dichloro(oxo)(diethyl malonate) vanadium(IV) [2]

Diethyl malonate (0.5 cm³, 3.3 mmol) was added dropwise to VOCl₃ (2 cm³, 21.1 mmol) in 50 cm³ of hexane and stirred under nitrogen for 2 h. An excess of VOCl₃ was used to ensure completion as unreacted VOCl₃ is facile to remove from the reaction. A very dark precipitate was formed in a dark red solution. The precipitate was filtered and washed 3 times with 20 cm³ hexane and dried *in vacuo* to afford **2** in good yield (0.9 g, 78%). Some of the product was re-dissolved in 5 cm³ dichloromethane and layered with 15 cm³ hexane. Small crystals formed over approximately one week. ¹H NMR (CDCl₃): δ 1.34 (t, 6H, -CH₃, *J* = 7.25 Hz, 3.35 (s, 2H, -CH₂)), 4.18 (q, 4H, -CH₂, *J* = 7.25 Hz). ¹³C {¹H} NMR (CDCl₃): δ 14.2 (CH₃), 55.9 (CH₂), 63.6 (CH₂CH₃), 163 (C=O). Elemental analysis calculated for C₇H₁₂O₅Cl₂V: C, 28.21; H, 4.06. Found: C, 26.38; H, 3.78.

2.3. Synthesis of dichloro(oxo)(diethyl succinate) vanadium(IV) [3]

Diethyl succinate (0.5 cm³, 3.3 mmol) was added dropwise to VOCl₃ (2 cm³, 21.1 mmol) in 40 cm³ of *n*-hexane and stirred under nitrogen for 2 h. A dark red solution formed immediately but no precipitate was observed. The product was dried *in vacuo* leading to the removal of the solvent and VOCl₃, leaving a viscous red liquid product (0.8 g, 90%). The flask containing the liquid product was left on its side for two weeks. Small green crystals were observed in the flask. ¹H NMR (CDCl₃): δ 1.21 (b, 6H, -CH₃), δ 2.59 (b, 4H, -CH₂CH₂), δ 4.12 (b, 4H, -CH₂CH₃). ¹³C {¹H} NMR (CDCl₃): δ 14.3 (CH₃), 29.2 (CH₂CH₂), 60.9 (CH₂CH₃), 173 (C=O). Elemental analysis calculated for C₈H₁₄O₅Cl₂V: C, 30.79; H, 4.52. Found: C, 29.83; H, 4.49.

2.4. Synthesis of vanadium nitride and carbide powders

Vanadium nitride and carbide powders were synthesised by weighing out ~0.2 g of compounds **1**, **2** and **3** in a nitrogen filled glovebox onto ceramic bricks. The samples were sealed with a layer of laboratory film before removal from the glovebox. The samples were then transferred immediately to a tube furnace. The samples were purged with a flow of nitrogen (for VN, BOC, 99.9%) or argon (for VC, BOC “pureshield” 99.9%) at room temperature for 30 min (flow rate 40 sccm) before heating to 1200 °C (heating rate 20 °C min⁻¹) for 24 h. The samples were then cooled to room temperature naturally. Gas flow was maintained throughout.

3. Instrumentation

Transmission electron microscopy (TEM) images were obtained using a high resolution TEM Jeol 2100 with a LaB₆ source operating at an acceleration voltage of 200 kV. Images were recorded on a Gatan Orius Charge-coupled device (CCD). Samples were prepared by drop-casting a sonicated dispersion of VN/VC in *n*-hexane onto a 400 mesh gold grid with a thin holey carbon film (Agar Scientific). Energy dispersive X-ray spectra (EDS) were recorded on an Oxford Instruments XMax EDS detector running AZTEC software. XRD patterns were carried out using a Stoe (Mo) StadiP diffractometer with a Mo X-ray source (Mo tube 50 kV 30 mA), monochromated (Pre-sample Ge (111) monochromator selects Kα1 only) and a Dectris Mython 1k silicon strip detector covering 18° 2θ. Samples were run in transmission mode, with the sample under rotation in the X-ray beam. All diffraction patterns obtained were compared with database standards. X-ray photoelectron spectroscopy was conducted on a Thermo Scientific K-alpha spectrometer with

monochromated Al Kα radiation, a dual beam charge compensation system and constant pass energy of 50 eV (spot size 400 μm). Survey scans were collected in the binding energy range 0–1200 eV. High-resolution peaks were used for the principal peaks of V (2p), O (1s), and C (1s). CASA XPS software was used to fit data, with a doublet separation of 7.5 eV used for V 2p [57].

4. Crystallography

Single crystal XRD was carried out by selecting a suitable crystal and mounting it on a nylon loop. The datasets of all three compounds were collected on a SuperNova, Dual, Cu, Atlas diffractometer. The crystal was kept at 150(1) K during data collection (with the exception of **2** which was collected at 77 K). All compounds were solved using Olex2 [58], the structure was solved with the olex2.solve [59] structure solution program using Charge Flipping and refined with the ShelXL [60] refinement package using Least Squares minimisation. All structures have been submitted to the CCDC; compound **1** CCDC 1030431, compound **2** CCDC 1033676, compound **3** CCDC 1033740.

5. Results and discussion

Excess vanadium(V) oxytrichloride was reacted with the bidentate dicarbonyl ligands; 2,4-pentanedione, diethyl malonate and diethyl succinate in anhydrous *n*-hexane under an atmosphere of nitrogen (Fig. 1). The reactions yielded a monomeric species, an oxo-bridged tetramer and a one dimensional coordination polymer respectively.

5.1. Dichloro(oxo) (2,4-pentanedione) vanadium(V) [VOCl₂(acac)] [1]

Excess VOCl₃ was reacted with 2,4-pentanedione (acacH) and stirred for 2 h under a nitrogen environment. A dark precipitate in a dark red solution formed immediately but the mixture was stirred for 2 h to ensure a full reaction. The dark purple product, [VOCl₂(acac)] [1], was dissolved in dichloromethane and layered with hexane. After a week small dark black crystals were observed which were suitable for single crystal X-ray crystallography. The crystal structure for compound **1** is shown in Fig. 2 along with crystallographic data and selected bond lengths and angles in Tables 1 and 2.

¹H NMR of **1** showed a peak at 2.39 ppm corresponding to the methyl groups on the acac ligand, which was upfield to the same peak, observed at 2.2 ppm, in uncoordinated acacH. In the ¹H NMR spectrum of **1** only one further peak was observed at 6.13 ppm. The integral of this peak has a 6:1 ratio with the peak corresponding to the two methyl

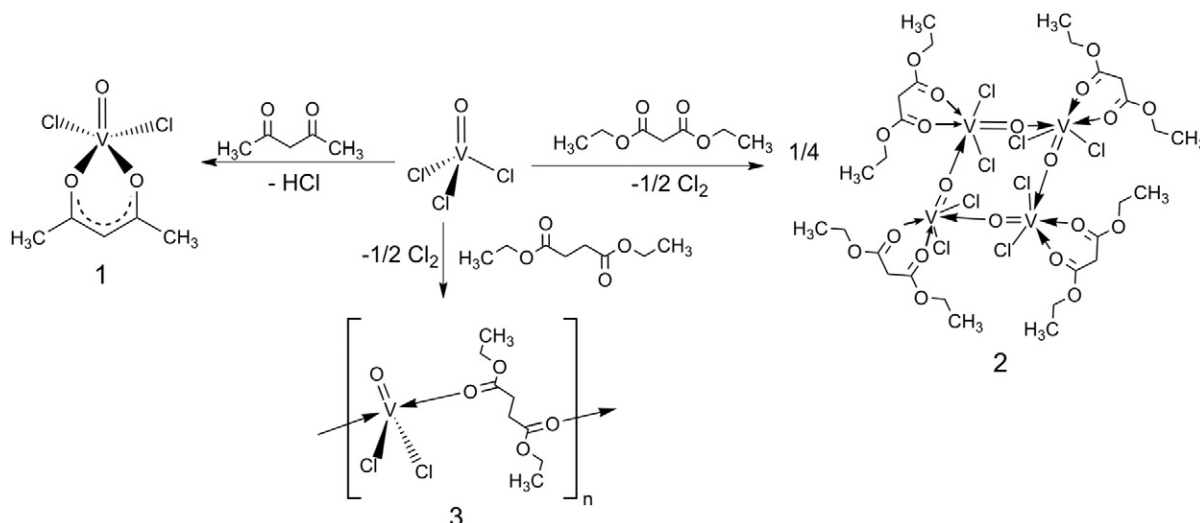


Fig. 1. Schematic reaction of excess VOCl₃ with diethyl malonate, 2,4-pentanedione and diethyl succinate in *n*-hexane to form compounds **1**, **2** and **3** respectively.

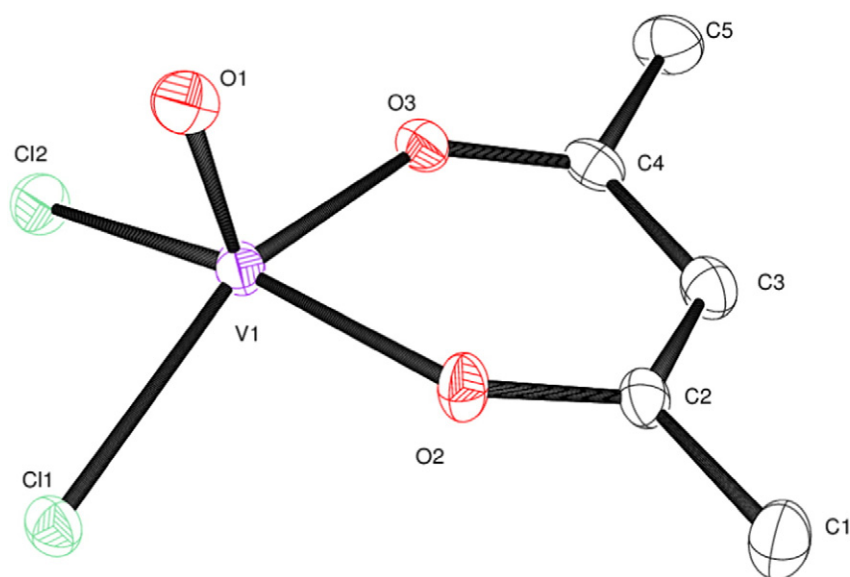


Fig. 2. ORTEP representation of crystal structure of $[\text{VOCl}_2(\text{acac})]$ [1] with thermal ellipsoids at the 50% probability level. Hydrogen atoms are omitted for clarity.

groups at 2.39 ppm. This provides clear evidence that one proton from the acac ligand has been lost on coordination to the vanadium centre with a concordant upfield chemical shift of 0.7 ppm. This suggests that the reaction of VOCl_3 with acacH proceeds *via* loss of HCl, as shown in Scheme 1.

The structure of compound **1**, which crystallises in the space group $P2_12_12_1$, shows that the acac ligand is bound to the vanadium centre *via* the carbonyl oxygen atoms. The V—O bond lengths are 1.903(2) Å for O(2) and 1.918(2) Å for O(3). These are shorter than typical dative V—O bond distances of ~2.1 Å, as described for **2** and **3** (*vide infra*) and is the result of the increased electron density given from the carbonyl oxygen. A proton from C(3) was lost in the reaction and a delocalised system is therefore created between O(3), C(2), C(3), C(4) and O(2).

This results in the ligand having an overall negative charge, which is stabilised by the reaction with the VOCl_3 resulting in a stronger bond to the vanadium than seen in complexes of VOCl_3 with the diesters, diethyl malonate and diethyl succinate (*vide infra*). This is evidenced in the crystal structure of **1** in which, the C2—C3 and C3—C4 bonds between the carbonyl groups appear shortened (1.398(4) Å and 1.383(4) Å respectively) [61]. This shows that the central carbon has been deprotonated leading to a conjugated 6 membered ring system as is frequently seen with coordination compounds of acac [62].

Compound **1** is five coordinate, which is common for vanadium species, particularly when a V=O bond is present. This is also seen for $[\text{VO}(\text{acac})_2]$, a five coordinate species in which the 4 carbonyl oxygen

atoms take an almost planar geometry with the double bond perpendicular [63]. In the case of compound **1**, the geometry is similar, with bond angles between the oxygen atoms in the acac O(2)—V(1)—O(3) at 84.62(9)°, whereas the angle between the chlorine atoms and the equivalent oxygen atoms on the acac are wider, at 86.65(7)° and 88.12(7)°, respectively for O(2)—V(1)—Cl(1) and O(3)—V(1)—Cl(2). The angle between the two chlorines (Cl(1)—V(1)—Cl(2)) is widest at 93.45(3)°. This is due to the increased repulsion between the chlorine atoms due to their greater size.

5.2. Dichloro(oxo) (diethyl malonate) vanadium(IV) $[\text{VOCl}_2(\text{CH}_2(\text{CO}_2\text{Et})_2)_4]$ [2]

Diethyl malonate was reacted with an excess of VOCl_3 at room temperature, which yielded dark red crystals of $[\text{VOCl}_2(\text{CH}_2(\text{CO}_2\text{Et})_2)_4]$ [2] after layering a concentrated solution of **2** in dichloromethane with hexane. NMR spectroscopy displayed strong peak broadening confirming the presence of a paramagnetic vanadium species. The ^1H NMR spectra of compound **2** show that peaks corresponding to the coordinated ligand have shifted downfield compared with that of the unreacted malonate starting material. The protons on the central carbon showed the greatest shift, implying they are most heavily deshielded by the presence of the vanadium, with the signal shifting downfield to 3.5 ppm from 3.2 ppm for the unreacted ligand.

Single crystal X-ray diffraction analysis of the red crystals revealed that the tetrameric complex $[\text{VOCl}_2(\text{CH}_2(\text{CO}_2\text{Et})_2)_4]$ [2] had formed, crystallising in the $P\bar{1}$ space group as shown in Fig. 3. The crystal structure of compound **2** is a tetramer linked by four bridging μ_2 -oxygen atoms. From each of the bridged vanadium centres a chlorine atom has been lost and the coordination sphere filled with the bridging V—O bond. Around each vanadium there are 4 V—O bonds. The two longest bonds are the dative bonds to the carbonyl groups of the diethyl malonate. These are similar to the equivalent Ti—O bond lengths (2.112(4) Å and 2.102(4) Å) observed for the same malonate ligand coordinating to titanium tetrachloride [64,65]. In the case of the TiCl_4 however, all four chlorides are retained, giving a monomeric species. The formation of tetrameric clusters has been observed previously in vanadium oxide chemistry when bidentate ligands are used [66]. The V=O bond is able to stabilise another unstable centre by coordinating to the vanadium to give an octahedral species, following the loss of chloride. It is possible that acac does not follow this motif due to the

Table 1
Crystallographic data for compounds 1–3.

Ligand	[1] $\text{VOCl}_2(2,4\text{-pentanedione})$	[2] $[\text{VOCl}_2(\text{diethyl malonate})]_4$	[3] $[\text{VOCl}_2(\text{diethyl succinate})]_n$
Crystal system	Orthorhombic	Triclinic	Monoclinic
Space group	$P2_12_12_1$	P-1	$P2_1/c$
<i>a</i>	8.3503(3) Å	12.5230(2) Å	15.3393(8) Å
<i>b</i>	13.5046(4) Å	13.3895(2) Å	9.7939(5) Å
<i>c</i>	15.2041(5) Å	17.5946(3) Å	8.6842(5) Å
α	90.000(5)	85.7322(14)	90
β	90.000(5)	84.0193(14)	94.664(5)
γ	90.000(5)	73.5084(15)	90
Volume/Å ³	1714.52(9)	2810.34(9)	1300.32(12)
Final R indices [$I \geq 2\sigma(I)$]	R1 = 0.0326 wR2 = 0.0647	R1 = 0.0551 wR2 = 0.1521	R1 = 0.0340 wR2 = 0.0746

Table 2
Selected bond lengths and angles for compounds **1–3**.

Compound	Selected bond lengths Å			Selected bond angles °				
[1]	V1–Cl1	2.2880(8)	O2–C2	1.290(4)	Cl2–V1–Cl1	93.45(3)	O2–V1–Cl2	159.64(7)
	V1–Cl2	2.2275(9)	O3–C4	1.283(4)	O1–V1–Cl1	99.58(9)	O2–V1–O3	84.62(9)
	V1–O1	1.569(2)	C2–C3	1.398(4)	O1–V1–Cl2	99.94(9)	O2–V1–Cl1	86.65(7)
	V1–O2	1.903(2)	C3–C4	1.383(4)	O1–V1–O2	100.11(10)	O3–V1–Cl2	88.12(7)
	V1–O3	1.918(2)			O1–V1–O3	101.11(10)	C2–O2–V1	134.21(19)
[2]	V1–O1	2.077(3)	C3–C4	1.498(7)	O1–V1–Cl2	89.07(10)	O4–V1–O1	83.64(13)
	V1–O2	2.148(3)	C4–C5	1.492(7)	O1–V1–O2	80.58(12)	O4–V1–O2	78.95(12)
	V1–O3	1.623(3)	C6–C7	1.496(9)	O3–V1–O1	93.47(14)	C3–O1–V1	133.1(3)
	V1–O4	2.036(3)	V1–Cl1	2.3031(13)	O3–V1–O2	171.21(15)	V2–O4–V1	174.44(19)
	V4–O3	2.027(3)	V1–Cl2	2.3023(14)	Cl1–V1–Cl2	93.66(5)	V1–O3–V4	172.1(2)
	O2–C5	1.222(6)						
[3]	V1–Cl1	2.2854(6)	O1–C3	1.228(2)	Cl2–V1–Cl1	131.62(3)	O2 ¹ –V1–Cl2	86.74(4)
	V1–Cl2	2.2776(6)	O4–C3	1.312(2)	O3–V1–Cl1	113.26(6)	C3–O1–V1	142.20(13)
	V1–O3	1.5783(14)	O2–C6	1.237(2)	O3–V1–O1	93.40(7)	C3–C4–C5	113.60(16)
	V1–O1	2.0483(13)	O5–C6	1.312(2)	O3–V1–O21	98.62(6)	O2 ¹ –V1–O1	167.72(6)
	V1–O21	2.0370(13)	O5–C7	1.473(2)	O1–V1–Cl2	85.88(4)		
	C3–C4	1.487(3)	C4–C5	1.530(3)				

¹ +X,+Y,1+Z

difference in the nature of bonding to the vanadium centre, with **1** having undergone the loss of a proton the central carbon giving rise to a delocalised structure that stabilised the monomeric species [67].

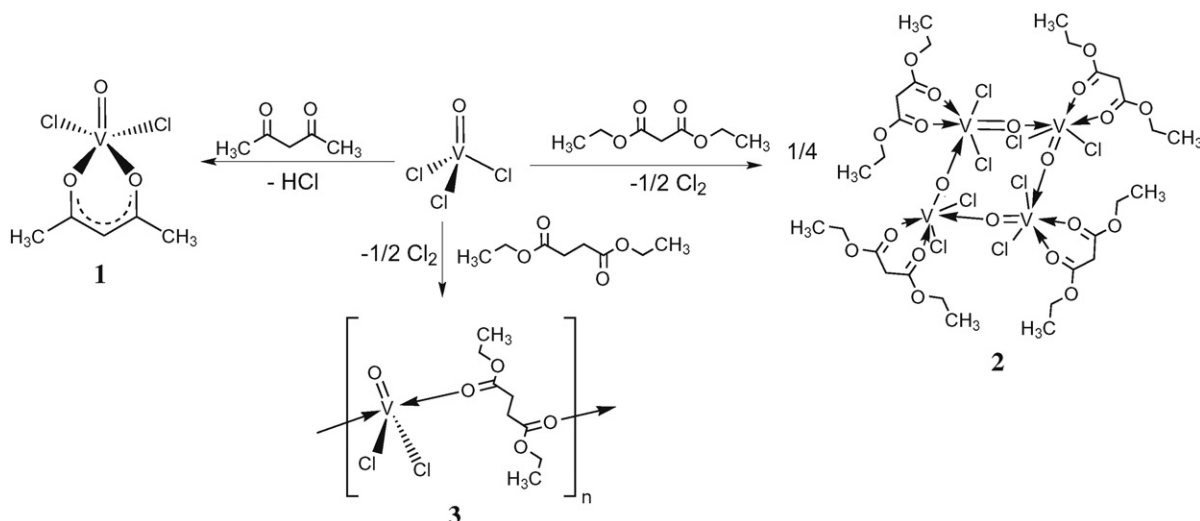
The other two V–O bond lengths represent the bridging oxygen bonds, this shows that the oxygen atom does not sit equidistant between the two vanadium atoms. The shorter of the two has a length of 1.623(3) Å, close to that expected for a V=O bond, for example 1.595(5) Å observed in VOCl₃ [68]. The other bridging V–O bond distance was considerably longer at 2.036(3) Å, resembling the dative coordination of the malonate. This shows that the original V=O bond in the VOCl₃ has not been broken but datively coordinates to another vanadium atom. This structure has been reported previously by Sobota et al. formed *via* accidental exposure to air of [V₂(μ-Cl)₂Cl₄{CH₂(CO₂Et)₂}₂] as formed from substitution of MeCO₂Et by diethyl malonate in [V₂(μ-Cl)₂Cl₄(MeCO₂Et)₄] [69]. Herein, however a direct route to **2** is reported.

Whilst **2** is the same the structure reported by Sobota et al. [69], with similar R factors (4.94% *cf.* 5.51%), the crystallographic data differs, which is likely a result of collection temperature (283–303 K *cf.* 77 K). This in turn has resulted in a better data set (Sobota structure has the unit cell dimensions: *a* = 12.655(4) Å, *b* = 13.735(3) Å, *c* = 18.141(3) Å, compared with: *a* = 12.5230(2) Å, *b* = 13.3895(2) Å,

c = 17.5946(3) Å, reported here). The low temperature collection reported here has been submitted to the CCDC since there are noticeable differences in the majority of the bond lengths and angles of the two structures and we consider this of interest to the field. For example the V–O bond distance between the vanadium and the carbonyl groups on the malonate is 2.177(6) Å in the previously reported structure, but is shorter in this case at only 2.077(3) Å. These differences are probably largely the result of the previous structural data being collected at room temperature, whereas in this study, crystals were analysed at 77 K.

Dimeric oxo-bridged vanadium complexes have been produced in a similar way by reaction of VOCl₃ and pinacol. In this case one of the oxygen atoms of each pinacol ligand was coordinated to both vanadium centres, acting as bridges, with the other oxygen coordinating to one [70]. The V–O bond lengths observed for the bridging oxygen atoms were 2.036(3) Å, resembling the dative coordination of the malonate, rather than a direct oxo bridge. This is likely due to the electron deficient nature of the vanadium centre. The dative V–O bond length of 2.036(3) Å in **2** is still shorter than the V–Cl bonds at 2.3031(13) Å.

In compound **2**, each of the vanadium atoms are coordinated to two chlorine atoms, having lost one on coordination to the ligand. The lengths of the C–C bonds between the two carbonyl groups are 1.492(7) and 1.498(7) Å which indicates that both are single bonds



Scheme 1. Schematic reaction of excess VOCl₃ with diethyl malonate, 2,4-pentanedione and diethyl succinate in *n*-hexane to form compounds **1**, **2** and **3** respectively.

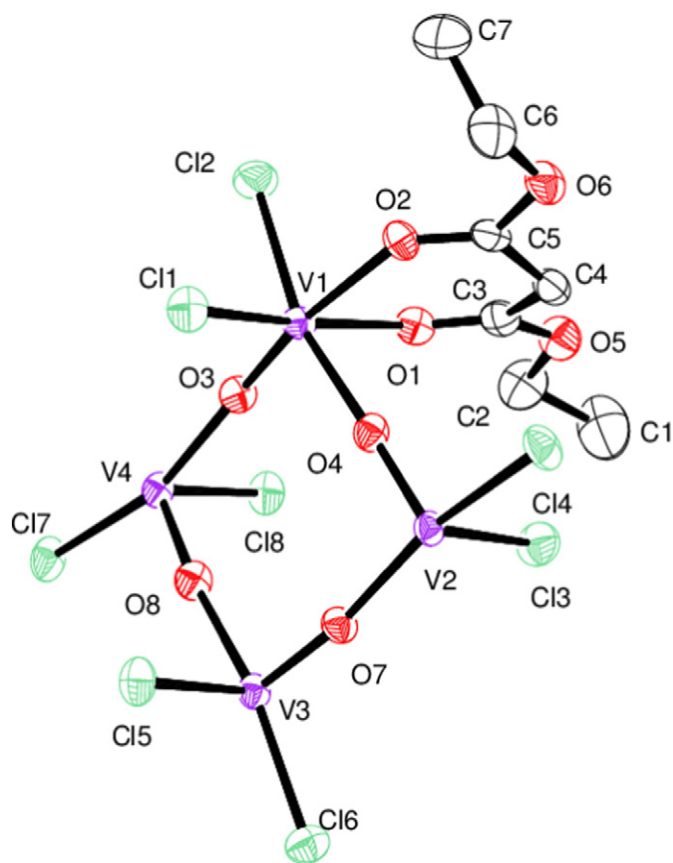


Fig. 3. ORTEP representation of crystal structure of $[\text{VOCl}_2(\text{CH}_2(\text{CO}_2\text{Et})_2)_4]$ **[2]** with thermal ellipsoids at the 50% probability level. Three of the four diethyl malonate molecules and all hydrogen atoms omitted for clarity.

[61]. This implies coordination to the vanadium centre has not led to the loss of a proton from the central carbon atom resulting in the evolution of HCl as would be expected and observed in the formation of compound **1**. Had this occurred the C—C bond lengths would be shortened to around 1.38 Å due to the increased electronic density resulting from the aromaticity of the resulting species. Therefore, the vanadium centre has been reduced to V(IV) from V(V) with concurrent oxidation of chloride ligands to elemental chlorine. This has been observed previously in the reaction of VOCl_3 with 2-ethoxy ethanol, which was shown to coordinate in a bidentate fashion to the vanadium whilst maintaining the ethanoic proton [71]. This reaction was found to result in the reversible loss of chlorine ligands *via* oxidation to Cl_2 . Vapours from the reaction were found to test positive for Cl_2 gas [71].

The formation of tetrameric clusters has been observed previously in vanadium oxide chemistry when bidentate ligands are used. The V=O bond is able to stabilise another unstable centre by coordinating to the vanadium to give an octahedral species, following the loss of chloride. It is possible that acac does not follow this motif due to the difference in the nature of bonding to the vanadium centre, with acac having undergone the loss of a proton the central carbon giving rise to a delocalised structure that stabilised the monomeric species.

5.3. Dichloro(oxo)(diethyl succinate) vanadium(IV) $[\text{VOCl}_2\{\text{C}_2\text{H}_4(\text{CO}_2\text{Et})_2\}]_n$ **[3]**

Excess VOCl_3 was reacted with diethyl succinate in hexane and stirred for 2 h under nitrogen. The reaction mixture turned from orange to dark red over 5 min and was left to stir for 2 h to ensure a complete reaction. The reaction yielded a dark red oily product (Fig. 1). The flask was left under nitrogen for one month, during which time green

crystals of compound **3** were formed which were suitable for single crystal X-ray crystallography.

The diethyl succinate acts as a bidentate ligand in **3**, with each carbonyl binding to a different metal centre rather than chelating as was observed with the malonate ligand in compound **2**, which crystallised in the space group $P2_1/c$. Likewise, each vanadium centre forms bonds with two different ester groups, forming a polymer chain. This polymer chain is classed as a one dimensional coordination polymer. Coordination polymers are metal-ligand complexes that extend “indefinitely” into one, two or three dimensions *via* covalent metal-ligand bonding. Coordination polymers are also known as metal organic frameworks (MOFs) [72,73]. One dimensional coordination polymers are of particular interest for their electronic properties, for use as nano-wires [74].

The first non-cluster vanadium coordination polymer was synthesised by Zhang et al. in 2001, with the synthesis of $[\text{VO}(\text{dod})_2]\text{X}_2$ ($\text{X} = \text{Cl}, \text{Br}$; $\text{dod} = 1,4$ -diazoniabicyclo [2,2,2]octane-1,4-diacetate) [75]. There have been two reported 1-dimensional coordination polymers containing vanadium, one with *O,O,N*-chelating ligands [76] and the other with bidentate ligands coordinating *via* oxygen atoms forming the bridge, stabilised by *N,N*-chelating terephthalate ligands [73]. Furthermore, succinate has been used as a bridging ligand in a cobalt based MOF, forming a similar one dimensional chain, stabilised with benzidine ligands [77].

This is to our knowledge, the first mononuclear 1-dimensional vanadyl coordination polymer to be isolated as a single crystal and the structure probed by X-ray diffraction. The presence of the two V—Cl bonds makes the polymer extremely moisture sensitive. The vanadium centre is similar to that in **1** in that it is five coordinate, bound to three oxygen atoms and two chlorine atoms. The complexes differ in the way that the ligand is oriented. In compound **1**, the carbonyl oxygen atoms are *cis* to each other since they are from the same acac ligand. In compound **3**, the carbonyl oxygen atoms originate from two different molecules and are positioned axial to each other, rather than basal, as in the case for **1**. This is reflected in the $\text{O}(1)\text{—V}(1)\text{—O}(21)$ bond angle of $167.72(6)^\circ$ in **3**, whereas in compound **1** the equivalent O—V—O angle between the carbonyl oxygen atoms is $84.62(9)^\circ$.

Structure **3** differs from the related cobalt polymer synthesised by Roy et al. [77], since the O—M—O bond angle was observed to be 180° . This is due to the electronegativity of the two chloride ligands, resulting in the $\text{Cl}(1)\text{—V}(1)\text{—Cl}(2)$ bond angle being $131.62(3)^\circ$, as opposed to the expected 120° for a five coordinate geometry. Regardless of this the chain is linear due to the positioning of the succinate bridge.

The V—O bond lengths in **3** for the carbonyl oxygen atoms are $2.0483(13)$ Å and $2.0370(13)$ Å respectively, which resembles the dative coordinative bonds observed with the malonate ligand in **2**. It is likely that **3** forms this polymer because of the two bridging carbon atoms between the ester groups. When there is one bridging carbon, as is the case with the malonate and the acac, both of the ketones lie on the same side of the chain. In the case of the succinate ligand there are two bridging carbon atoms, the bond between which can rotate freely, allowing the carbonyls to lie on opposite sides due to steric hindrance. Furthermore, the thermodynamics of 6-membered ring formation is more favourable than 7-membered ring formation, hence ligand acts as a bridge (Fig. 4).

Each of the diester molecules were observed to have dative coordination to the vanadium metal centre, facilitated by the loss of a molecule of chlorine, as was observed for compound **2**. The structures differ greatly according to the ligand, with the malonates appearing to favour oxo-bridged oligomeric structures, whilst the less oxygen rich acac favours a simple monomeric species.

Another interesting characteristic of the diester species is that both the NMR spectra and bond lengths observed suggests that there is no deprotonation of the ligand to form a conjugated species, as is observed in the acac ligand. This may relate back to the propensity for forming oligomeric and polymeric species, which could facilitate the loss of Cl_2

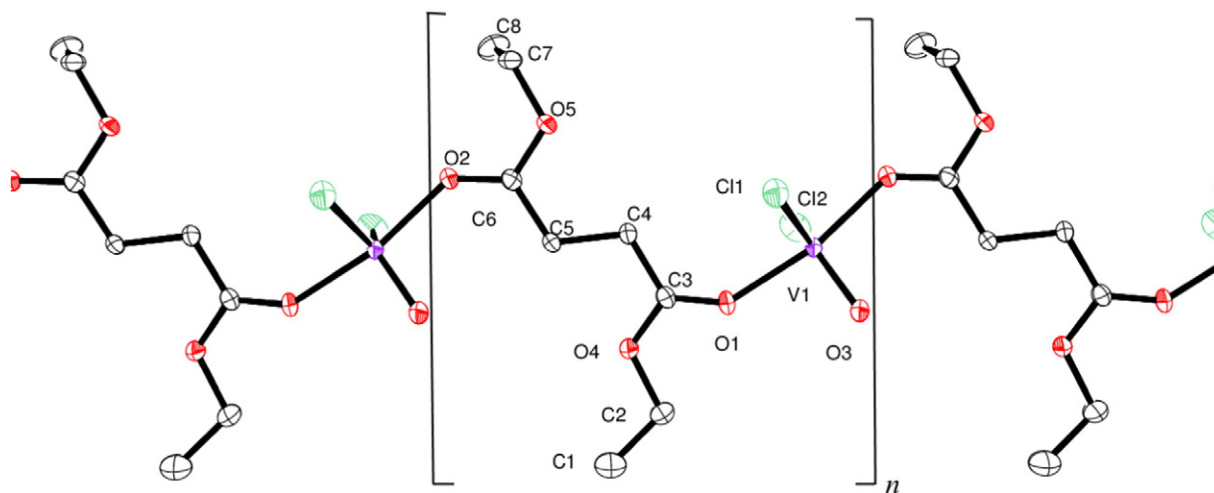


Fig. 4. ORTEP representation of crystal structure of $[\text{VOCl}_2(\text{C}_2\text{H}_4(\text{CO}_2\text{Et})_2)]_n$ [3] with thermal ellipsoids at the 50% probability level. Hydrogen atoms are omitted for clarity.

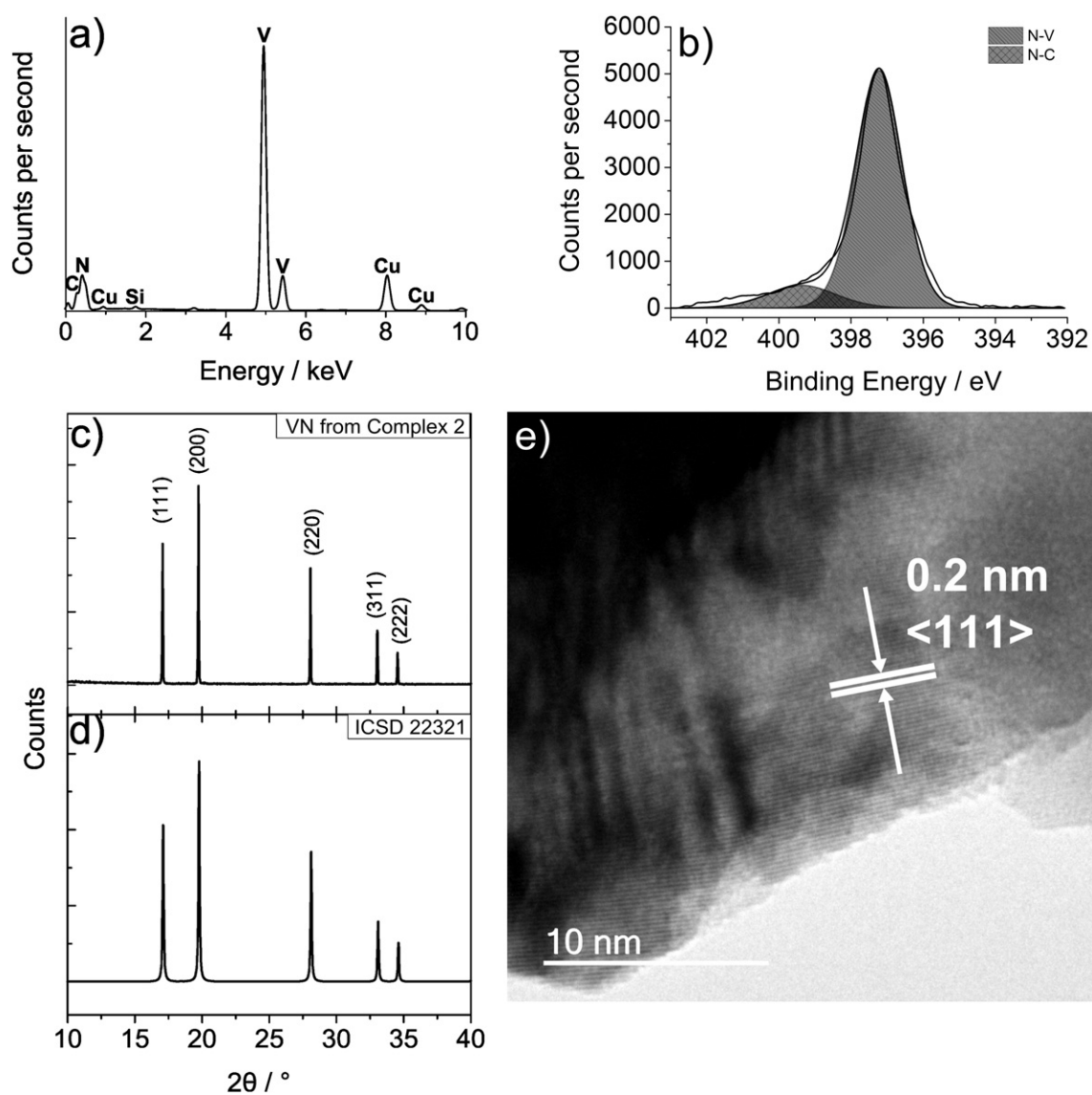


Fig. 5. Composite figure for the VN sample derived from complex 2. a) shows an EDS spectrum demonstrating the presence of vanadium and nitrogen with little carbon present. Copper emanated from the copper mesh TEM grid. b) Fitted N1s XPS spectrum showing the regions assigned as VN and VC. c) and d) show XRD patterns of VN derived from complex 2 compared to a VN ICSD standard (22321). e) is an HRTEM image of a VN crystal with the $\langle 111 \rangle$ plane of VN highlighted.

gas in the event of the dimerization of two unstable vanadium centres as a preferable reaction pathway [71].

5.4. Synthesis and characterisation of vanadium nitride powders

Vanadium nitride powders were synthesised by annealing compounds **1**, **2** and **3** under nitrogen gas.

flow at 1200 °C for 24 h. It is necessary to treat vanadium species at such high temperatures to illicit the formation of vanadium nitride due to the intrinsic stability of various vanadium oxides such as V_2O_5 . All compounds produced a grey powder containing gold flecks. Compounds **1**, **2** and **3** showed near complete transformation to vanadium nitride at 1200 °C as evidenced by the XRD patterns in Fig. 5c) and d) and Fig. S5, ESI. The XRD patterns were compared to a VN standard (ICSD 22321), all samples were shown to be phase pure with only diffraction peaks for VN visible. For the $VN_{1.00}$ unit cell, the total calculated volume is $566.8 \pm 2 \text{ \AA}^3$ (a 0.35% maximum error), which compares with the ICSD standard of 567.5 \AA^3 - a difference of 0.117%. Ortega et al. [78] determined the reaction mechanism for the reaction of vanadium(III) oxide (V_2O_3) and carbon in the presence of nitrogen gas at elevated

temperatures (up to 1180 °C). Nitridation was simultaneous with carbothermal reduction, from V_2O_3 to V_8C_7 to VN, and was completed at lower temperatures than just V_2O_3 in nitrogen. Compounds **1**, **2** and **3** decomposed in nitrogen gas is similar to this system due to the presence of oxygen and carbon in the compounds. Ortega et al. [79] followed the progress of the reaction of by measuring the partial pressures of evolved carbon monoxide, supporting the V_2O_5 - V_2O_4 - VO_2 - V_2O_3 - $VO_{0.9}$ -VN pathway, despite the difficulty in the detection of $V_{0.9}$.

XPS analysis, (Figs. 5b) and S6, showed the presence of vanadium nitride in both the N1s and V2p_{3/2} at 397.2 and 513.6 eV respectively. These match exactly with literature values [80]. The XPS also showed evidence for vanadium carbide and oxidised V^{5+} . The carbide was likely due to excess carbon presence in the precursor and the V^{5+} signal is typical for surface bound oxygen in vanadium surfaces and from the oxygen containing precursors themselves [66,81].

TEM analysis of all VN samples showed the formation of large, poly-disperse crystallites of VN (42.9 nm (sample derived from 1), 88.4 nm (sample derived from 2) and 72.4 nm (sample derived from 3)). Small amounts of crystalline carbon was also present around the edges of the VN crystallites, a consequence of carbonaceous ligands present in

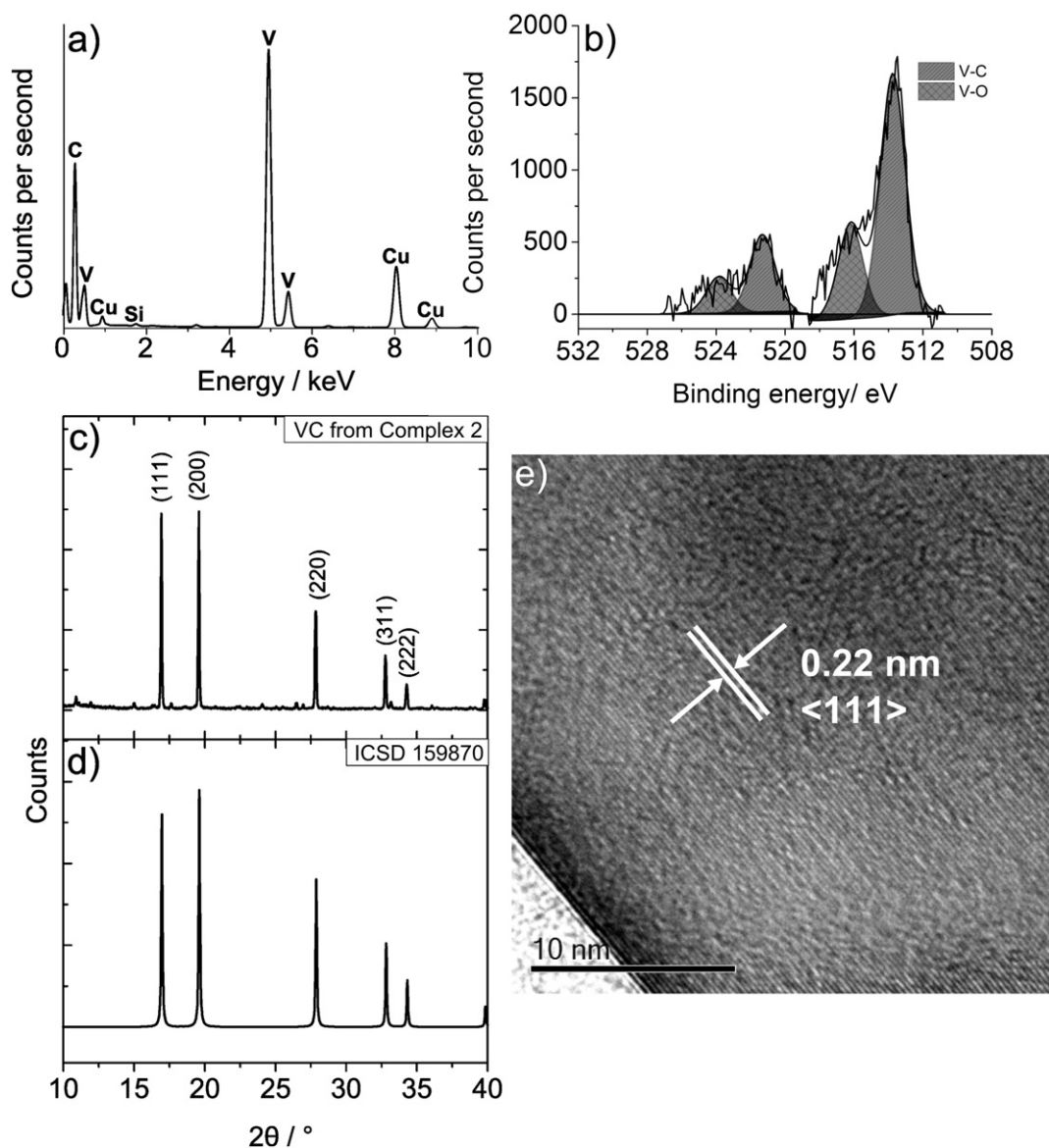


Fig. 6. Composite figure for the VC sample derived from complex 2. a) shows an EDS spectrum demonstrating the presence of vanadium and high levels of carbon. Copper emanated from the copper mesh TEM grid. b) Fitted V2p XPS spectrum showing the regions assigned as VC and VO. c) and d) show XRD patterns of VC derived from complex 2 compared to a VC ICSD standard (159870). e) is an HRTEM image of a VC crystal with the $\langle 111 \rangle$ plane of VC highlighted.

the initial complexes. In some cases, this was observed as a coating around the VN (see Fig. S1, ESI a)). HRTEM analysis of all samples demonstrated the presence of VN, via analysis of the *d*-spacings. Several *d*-spacings were indexed (Figs. 5e) and S1 b) and d), with the $\langle 111 \rangle$ plane of VN identified in all samples, with *d*-spacings from the samples derived from compounds **1**, **2** and **3**: 0.24 nm, 0.2 nm and 0.23 nm respectively and commensurate with obtained XRD patterns.

EDS analysis indicated the presence of nitrogen and vanadium with relatively low amounts of carbon (Figs. 5a) and S3 a) and c) in all samples analysed. Quantitative EDS analysis in all samples showed a ca. 50:50 at.% ratio, indicative of the formation of VN. The presence of residual carbon species presented difficulties in integrating the nitrogen peak as their EDS fingerprints appear in the same region of the spectrum. The relatively low amount of carbon in the sample (ca. 23% of total) compared to 88% in the equivalent VC sample and the large VN crystallites allowed for accurate confirmation of a 50:50 at.% ratio of V:N, and therefore confirmation of the VN empirical formula.

5.5. Synthesis and characterisation of vanadium carbide powders

Vanadium carbide powders were synthesised by annealing compounds **1**, **2** and **3** under an argon flow at 1200 °C for 24 h, yielding a black powder. There was evidence to show a transformation to VC under these conditions, however phase purity in compounds **1** and **3** was difficult to obtain (Fig. S6). The VC derived from compound **2** showed excellent conversion as evidenced by XRD analysis in Fig. 6c). It is noteworthy that lowering the temperature to 1000 °C under nitrogen induced compound's **1**, **2** and **3**'s transformation to VN but not to pure VC under Ar (Fig. S8). The XRD patterns were compared to a vanadium carbide standard (ICSD 159870), Fig. 6d). For the VC_{1.00} unit cell, the calculated total volume is $577.8 \pm 2 \text{ \AA}^3$ (a 0.35% maximum error), which compares with the ICSD standard of 578.8 \AA^3 , a % difference of 0.169%. As shown, the samples produced were phase pure, with only diffraction peaks for VC present in the patterns. Previous work by Nartowski et al. were able to demonstrate the synthesis of V₈C₇ powders by the reaction of VCl₃ and CaC₂ at 1000 °C for 2 days [82], but were unable to isolate phase pure VC_{1.00} using this route, showing the advantage of our single source precursor method. This is also supported by research from Kim et al. who synthesised V₈C₇ from the pyrolysis of the metal-organic framework MIL-47 at 1100 °C for 6 h [48].

XPS analysis (Figs. 6b) and S7, ESI) showed the presence of vanadium carbide in both the C1s and V2p_{3/2} at 282.8 and 513.7 eV respectively. These are in agreement with literature values [83]. The C1s showed several other environments, which were matched to C—C, C—O and C—OR— with these environments being more intense than the V—C signal. This was also reflected in the V2p signal, which was significantly weaker than the C1s, this was attributed to the formation of a carbon 'shell' around the VC particles during annealing.

TEM analysis of all VC samples showed the formation of large, poly-disperse crystallites of VC (111.7 nm (sample derived from **1**), 108.8 nm (sample derived from **2**) and 101.1 nm (sample derived from **3**) similar to those obtained for VN. A large amount of crystalline carbon was in evidence (Fig. S2 c)). HRTEM analysis of all samples demonstrated the presence of VN, via analysis of the *d*-spacings. Several *d*-spacings were indexed (Fig. 6e) and Fig. S2 b) and d) ESI, with the $\langle 111 \rangle$ plane of VC identified in all samples, with *d*-spacings from the samples derived from compounds **1**, **2** and **3**: 0.22 nm, 0.22 nm and 0.23 nm respectively, commensurate with obtained XRD patterns.

EDS analysis indicated the presence of carbon and vanadium with high amounts of carbon (Figs. 6a) and S3 b) and d) in all samples analysed. Quantitative EDS analysis showed a small difference in each of the samples. The sample derived from **1** showed a ca. 95:5 at.% ratio of C:V, the sample derived from **2** a ca. 90:10 at.% ratio, and the sample derived from **3** a ca. 85:15 at.% ratio. The carbon film on the TEM grid skews the ratio in favour of carbon, but the carbon-rich nature of the

structures produced was confirmed by quantitative XPS giving ratios of 94.3 carbon : 5.7 vanadium for the sample derived from **1**.

6. Conclusion

The crystal structures for complexes **1**, **2** and **3**, resulting from the reaction of the 2,4-pentanedione and diesters with the vanadium(V) oxytrichloride show different behaviour, from a monomer in **1**, a tetramer in **2**, to a 1D co-ordination polymer in **3**. With VOCl₃, all three molecules coordinating to the vanadium lead to the loss of a chlorine atom. This is significant as the reaction could not be reversed by simple dissociation of the ligand alone. To compensate for the loss of the chlorine atom, the diester complexes **2** and **3**, form a ring and a chain respectively, with the oxygen of the VOCl₃ forming a dative bond with another metal centre.

Complexes **1**, **2** and **3** were evaluated for their propensity to form VN and VC on annealing at 1200 °C under nitrogen and argon gas respectively. All samples converted to VN at 1200 °C under nitrogen, but complex **2** was the only molecule shown to be a viable precursor for both VC and VN. These complexes should therefore provoke further interest in the investigation of molecular species as precursors for hard materials.

Acknowledgements

The Engineering and Physical Sciences Research Council (EPSRC) and Huntsman Pigments are thanked for studentship funding (B. B.) through the Molecular Modelling and Materials Science Doctoral Training Centre (grant EP/G036675) and for grants EP/H00064X and EP/K001515. JCB and CEK acknowledge the Ramsay Memorial Trust for Ramsay Fellowships.

Appendix A. Supplementary data

Supplementary data to this article can be found online at <http://dx.doi.org/10.1016/j.matdes.2016.06.029>.

References

- [1] P. Krawiec, S. Kaskel, Transition metal nitrides and carbides, in: K.J. Klabunde, R.M. Richards (Eds.), *Nanoscale Mater. Chem.* John Wiley & Sons, Inc. 2009, pp. 111–125, <http://dx.doi.org/10.1002/9780470523674.ch5/summary> (accessed January 21, 2016).
- [2] A. Morel, Y. Borjon-Piron, R.L. Porto, T. Brousse, D. Bélanger, Suitable conditions for the use of vanadium nitride as an electrode for electrochemical capacitor, *J. Electrochem. Soc.* 163 (2016) A1077–A1082, <http://dx.doi.org/10.1149/2.1221606jes>.
- [3] R. Franz, C. Mitterer, Vanadium containing self-adaptive low-friction hard coatings for high-temperature applications: a review, *Surf. Coat. Technol.* 228 (2013) 1–13, <http://dx.doi.org/10.1016/j.surfcoat.2013.04.034>.
- [4] S.V. Didziulis, K.D. Butcher, A perspective on the properties and surface reactivities of carbides and nitrides of titanium and vanadium, *Coord. Chem. Rev.* 257 (2013) 93–109, <http://dx.doi.org/10.1016/j.ccr.2012.04.015>.
- [5] L. Wu, T. Yao, Y. Wang, J. Zhang, F. Xiao, B. Liao, Understanding the mechanical properties of vanadium carbides: nano-indentation measurement and first-principles calculations, *J. Alloys Compd.* 548 (2013) 60–64, <http://dx.doi.org/10.1016/j.jallcom.2012.09.014>.
- [6] V.I. Stanciu, V. Vitry, F. Delaunois, Tungsten carbide powder obtained by direct carburization of tungsten trioxide using mechanical alloying method, *J. Alloys Compd.* 659 (2016) 302–308, <http://dx.doi.org/10.1016/j.jallcom.2015.10.265>.
- [7] I. Hussainova, Effect of microstructure on the erosive wear of titanium carbide-based ceramics, *Wear* 255 (2003) 121–128, [http://dx.doi.org/10.1016/S0043-1648\(03\)00198-4](http://dx.doi.org/10.1016/S0043-1648(03)00198-4).
- [8] R.H.J. Hannink, M.J. Murray, Elastic moduli measurements of some cubic transition metal carbides and alloyed carbides, *J. Mater. Sci.* 9 (1974) 223–228, <http://dx.doi.org/10.1007/BF00550945>.
- [9] K. Liu, X.P. Li, M. Rahman, X.D. Liu, CBN tool wear in ductile cutting of tungsten carbide, *Wear* 255 (2003) 1344–1351, [http://dx.doi.org/10.1016/S0043-1648\(03\)00061-9](http://dx.doi.org/10.1016/S0043-1648(03)00061-9).
- [10] C. Kral, W. Lengauer, D. Rafaja, P. Ettmayer, Critical review on the elastic properties of transition metal carbides, nitrides and carbonitrides, *J. Alloys Compd.* 265 (1998) 215–233, [http://dx.doi.org/10.1016/S0925-8388\(97\)00297-1](http://dx.doi.org/10.1016/S0925-8388(97)00297-1).
- [11] P. Muije, R.M. Horton, S.A. Duran, Kinetics of solid vanadium-nitrogen reactions at high temperatures, *Metall. Trans.* 5 (1974) 97–104, <http://dx.doi.org/10.1007/BF02642932>.

- [12] Y.I. Matrosov, V.N. Anashenko, Vanadium nitride in low-alloy low-carbon steels, *Met. Sci. Heat Treat.* 13 (1971) 893–896, <http://dx.doi.org/10.1007/BF00713836>.
- [13] D. Choi, G.E. Blomgren, P.N. Kumta, Fast and reversible surface redox reaction in nanocrystalline vanadium nitride supercapacitors, *Adv. Mater.* 18 (2006) 1178–1182, <http://dx.doi.org/10.1002/adma.200502471>.
- [14] T.S. Oyama, R. Kapoor, H.T. Oyama, D.J. Hofmann, E. Matijević, Topotactic synthesis of vanadium nitride solid foams, *J. Mater. Res.* 8 (1993) 1450–1454, <http://dx.doi.org/10.1557/JMR.1993.1450>.
- [15] J.-W. Huang, H. Peng, G.-B. Xia, Microwave synthesis of vanadium nitride for industrial applications, *Ironmak. Steelmak.* 36 (2009) 110–114, <http://dx.doi.org/10.1179/174328107X255005>.
- [16] B. Vaidhyanathan, D.K. Agrawal, R. Roy, Novel synthesis of nitride powders by microwave-assisted combustion, *J. Mater. Res.* 15 (2000) 974–981, <http://dx.doi.org/10.1557/JMR.2000.0139>.
- [17] B. Vaidhyanathan, K.J. Rao, Synthesis of Ti, Ga, and V nitrides: microwave-assisted carbothermal reduction and nitridation, *Chem. Mater.* 9 (1997) 1196–1200, <http://dx.doi.org/10.1021/cm9605835>.
- [18] T. Huang, S. Mao, G. Zhou, Z. Wen, X. Huang, S. Ci, J. Chen, Hydrothermal synthesis of vanadium nitride and modulation of its catalytic performance for oxygen reduction reaction, *Nanoscale* 6 (2014) 9608–9613, <http://dx.doi.org/10.1039/C4NR02646B>.
- [19] Y.C. Hong, D.H. Shin, H.S. Uhm, Production of vanadium nitride nanopowders from gas-phase VOCl_3 by making use of microwave plasma torch, *Mater. Chem. Phys.* 101 (2007) 35–40, <http://dx.doi.org/10.1016/j.matchemphys.2006.02.009>.
- [20] A. Newport, C.J. Carmalt, I.P. Parkin, S.A. O'Neill, Formation of VN from VCl_4 and $\text{NH}(\text{SiMe}_3)_2$ by APCVD – a potential solar control coating, *Eur. J. Inorg. Chem.* 2004 (2004) 4286–4290, <http://dx.doi.org/10.1002/ejic.200400344>.
- [21] I.P. Parkin, G.S. Elwin, Atmospheric pressure chemical vapour deposition of vanadium nitride and oxynitride films on glass from reaction of VCl_4 with NH_3 , *J. Mater. Chem.* 11 (2001) 3120–3124, <http://dx.doi.org/10.1039/B103843P>.
- [22] G. Hyett, M.A. Green, I.P. Parkin, An investigation of titanium–vanadium nitride phase space, conducted using combinatorial atmospheric pressure CVD, *Chem. Vap. Depos.* 14 (2008) 309–312, <http://dx.doi.org/10.1002/cvde.200806705>.
- [23] R. Fix, R.G. Gordon, D.M. Hoffman, Chemical vapor deposition of vanadium, niobium, and tantalum nitride thin films, *Chem. Mater.* 5 (1993) 614–619, <http://dx.doi.org/10.1021/cm00029a007>.
- [24] L. Chen, Y. Gu, L. Shi, Z. Yang, J. Ma, Y. Qian, A room-temperature synthesis of nanocrystalline vanadium nitride, *Solid State Commun.* 132 (2004) 343–346, <http://dx.doi.org/10.1016/j.ssc.2004.07.041>.
- [25] C. Giordano, C. Erpen, W. Yao, B. Milke, M. Antonietti, Metal nitride and metal carbide nanoparticles by a soft urea pathway, *Chem. Mater.* 21 (2009) 5136–5144, <http://dx.doi.org/10.1021/cm9018953>.
- [26] M. Wu, H. Guo, Y. Lin, K. Wu, T. Ma, A. Hagfeldt, Synthesis of highly effective vanadium nitride (VN) peas as a counter electrode catalyst in dye-sensitized solar cells, *J. Phys. Chem. C* 118 (2014) 12625–12631, <http://dx.doi.org/10.1021/jp501797e>.
- [27] J. Buha, I. Djerdj, M. Antonietti, M. Niederberger, Thermal transformation of metal oxide nanoparticles into nanocrystalline metal nitrides using cyanamide and urea as nitrogen source, *Chem. Mater.* 19 (2007) 3499–3505, <http://dx.doi.org/10.1021/cm0701759>.
- [28] J. Ma, M. Wu, Y. Du, S. Chen, J. Ye, L. Jin, Low temperature synthesis of vanadium carbide (VC), *Mater. Lett.* 63 (2009) 905–907, <http://dx.doi.org/10.1016/j.matlet.2009.01.033>.
- [29] C. Aguzzoli, C.A. Figueroa, F.S. de Souza, A. Spinelli, I.J.R. Baumvol, Corrosion and nanomechanical properties of vanadium carbide thin film coatings of tool steel, *Surf. Coat. Technol.* 206 (2012) 2725–2731, <http://dx.doi.org/10.1016/j.surfcoat.2011.11.042>.
- [30] M. Biesuz, V.M. Sglavo, Chromium and vanadium carbide and nitride coatings obtained by TRD techniques on UNI 42CrMoS₄ (AISI 4140) steel, *Surf. Coat. Technol.* 286 (2016) 319–326, <http://dx.doi.org/10.1016/j.surfcoat.2015.12.063>.
- [31] S. Gündüz, R.C. Cochrane, Influence of cooling rate and tempering on precipitation and hardness of vanadium microalloyed steel, *Mater. Des.* 26 (2005) 486–492, <http://dx.doi.org/10.1016/j.matdes.2004.07.022>.
- [32] V. Ollilainen, W. Kasprzak, L. Holappa, The effect of silicon, vanadium and nitrogen on the microstructure and hardness of air cooled medium carbon low alloy steels, *J. Mater. Process. Technol.* 134 (2003) 405–412, [http://dx.doi.org/10.1016/S0924-0136\(02\)01131-7](http://dx.doi.org/10.1016/S0924-0136(02)01131-7).
- [33] G. Yang, X. Sun, Z. Li, X. Li, Q. Yong, Effects of vanadium on the microstructure and mechanical properties of a high strength low alloy martensite steel, *Mater. Des.* 50 (2013) 102–107, <http://dx.doi.org/10.1016/j.matdes.2013.03.019>.
- [34] B. Chicco, W.E. Borbidge, E. Summerville, Experimental study of vanadium carbide and carbonitride coatings, *Mater. Sci. Eng. A* 266 (1999) 62–72, [http://dx.doi.org/10.1016/S0921-5093\(99\)00035-0](http://dx.doi.org/10.1016/S0921-5093(99)00035-0).
- [35] M. Aghaie-Khafri, F. Fazlalipour, Kinetics of V(N,C) coating produced by a duplex surface treatment, *Surf. Coat. Technol.* 202 (2008) 4107–4113, <http://dx.doi.org/10.1016/j.surfcoat.2008.02.027>.
- [36] J.B. Claridge, A.P.E. York, A.J. Brungs, M.L.H. Green, Study of the temperature-programmed reaction synthesis of early transition metal carbide and nitride catalyst materials from oxide precursors, *Chem. Mater.* 12 (2000) 132–142, <http://dx.doi.org/10.1021/cm9911060>.
- [37] S.M. Schmuecker, B.M. Leonard, Formation mechanism of nanostructured metal carbides via salt-flux synthesis, *Inorg. Chem.* 54 (2015) 3889–3895, <http://dx.doi.org/10.1021/acs.inorgchem.5b00059>.
- [38] F. Liu, Y. Yao, H. Zhang, Y. Kang, G. Yin, Z. Huang, X. Liao, X. Liang, Synthesis and characterization of vanadium carbide nanoparticles by thermal refluxing-derived precursors, *J. Mater. Sci.* 46 (2011) 3693–3697, <http://dx.doi.org/10.1007/s10853-010-5123-y>.
- [39] M. Mahajan, K. Singh, O.P. Pandey, Synthesis of vanadium carbide nanoparticles by thermal decomposition of the precursor, in: S. Bhardwaj, M.S. Shekhawat, B. Suthar (Eds.), *Proceeding Int. Conf. Recent Trends Appl. Phys. Mater. Sci. Ram 2013*, Amer Inst Physics, Melville 2013, pp. 271–272.
- [40] M. Mahajan, K. Singh, O.P. Pandey, Single step synthesis of nano vanadium carbide– V_8C_7 phase, *Int. J. Refract. Met. Hard Mater.* 36 (2013) 106–110, <http://dx.doi.org/10.1016/j.jirmhm.2012.07.009>.
- [41] Y. Chen, H. Zhang, H. Ye, J. Ma, A simple and novel route to synthesize nano-vanadium carbide using magnesium powders, vanadium pentoxide and different carbon source, *Int. J. Refract. Met. Hard Mater.* 29 (2011) 528–531, <http://dx.doi.org/10.1016/j.jirmhm.2011.03.004>.
- [42] L. Poirier, O. Richard, M. Ducarroir, M. Nadal, F. Teyssandier, F. Laurent, O. Cyr-Athis, R. Choukroun, L. Valade, P. Cassoux, Vanadocene used as a precursor for the chemical vapor deposition of vanadium carbide at atmospheric pressure, *Thin Solid Films* 249 (1994) 62–69, [http://dx.doi.org/10.1016/0040-6090\(94\)90086-8](http://dx.doi.org/10.1016/0040-6090(94)90086-8).
- [43] S.T. Oyama, *Chemistry of Transition Metal Carbides and Nitrides*, 1996 Edition, Springer, 1996.
- [44] G.M. Brown, L. Maya, Cyclopentadienylvanadium carbonyl derivatives as precursors to vanadium carbide, *Inorg. Chem.* 28 (1989) 2007–2010, <http://dx.doi.org/10.1021/ic00309a048>.
- [45] K. Dewangan, G.P. Patil, R.V. Kashid, V.S. Bagal, M.A. More, D.S. Joag, N.S. Gajbhiye, P.G. Chavan, V_2O_5 precursor-templated synthesis of textured nanoparticles based VN nanofibers and their exploration as efficient field emitter, *Vacuum* 109 (2014) 223–229, <http://dx.doi.org/10.1016/j.vacuum.2014.07.027>.
- [46] K.H. Lo, C.H. Shek, J.K.L. Lai, Recent developments in stainless steels, *Mater. Sci. Eng. R. Rep.* 65 (2009) 39–104, <http://dx.doi.org/10.1016/j.mser.2009.03.001>.
- [47] T. Sourmail, Precipitation in creep resistant austenitic stainless steels, *Mater. Sci. Technol.* 17 (2001) 1–14, <http://dx.doi.org/10.1179/026708301101508972>.
- [48] J. Kim, N.D. McNamara, J.C. Hicks, Catalytic activity and stability of carbon supported V oxides and carbides synthesized via pyrolysis of MIL-47 (V), *Appl. Catal. A Gen.* 517 (2016) 141–150, <http://dx.doi.org/10.1016/j.apcata.2016.03.011>.
- [49] E.F. de Souza, C.A. Chagas, T.C. Ramalho, R.B. de Alencastro, A versatile low temperature solid-state synthesis of vanadium nitride (VN) via a “guanidinium-route”: experimental and theoretical studies from the key-intermediate to the final product, *Dalton Trans.* 41 (2012) 14381–14390, <http://dx.doi.org/10.1039/C2DT31614E>.
- [50] T.C.M. Corbiere, D. Ressnig, C. Giordano, M. Antonietti, Focused radiation heating for controlled high temperature chemistry, exemplified with the preparation of vanadium nitride nanoparticles, *RSC Adv.* 3 (2013) 15337–15343, <http://dx.doi.org/10.1039/C3RA41040D>.
- [51] Z. Hou, K. Guo, H. Li, T. Zhai, Facile synthesis and electrochemical properties of nanoflake VN for supercapacitors, *CrystEngComm* 18 (2016) 3040–3047, <http://dx.doi.org/10.1039/C6CE00333H>.
- [52] P.J. Hanumantha, M.K. Datta, K.S. Kadakia, D.H. Hong, S.J. Chung, M.C. Tam, J.A. Poston, A. Manivannan, P.N. Kumta, A simple low temperature synthesis of nanostructured vanadium nitride for supercapacitor applications, *J. Electrochem. Soc.* 160 (2013) A2195–A2206, <http://dx.doi.org/10.1149/2.081311jes>.
- [53] E.F. de Souza, C.A. Chagas, T.C. Ramalho, V. Teixeira de Silva, D.L.M. Aguiar, R. San Gil, R.B. de Alencastro, A combined experimental and theoretical study on the formation of crystalline vanadium nitride (VN) in low temperature through a fully solid-state synthesis route, *J. Phys. Chem. C* 117 (2013) 25659–25668.
- [54] S.A. Hassanzadeh-Tabrizi, D. Davoodi, A.A. Beykzadeh, A. Chami, Fast synthesis of VC and V_2C nanopowders by the mechanochemical combustion method, *Int. J. Refract. Hard Mater.* 51 (2015) 1–5.
- [55] D. Xinhui, C. Srinivasakannan, Z. Hong, Z. Yuedan, Process optimization of the preparation of vanadium nitride from vanadium pentoxide, *Arab. J. Sci. Eng.* 40 (2015) 2133–2139, <http://dx.doi.org/10.1007/s13369-015-1763-1>.
- [56] A.B. Pangborn, M.A. Giardello, R.H. Grubbs, R.K. Rosen, F.J. Timmers, Safe and convenient procedure for solvent purification, *Organometallics* 15 (1996) 1518–1520, <http://dx.doi.org/10.1021/om9503712>.
- [57] NIST X-ray Photoelectron Spectroscopy (XPS) Database, version 3.5, NIST X-Ray Photoelectron Spectrosc. XPS database version 35(n.d.) <http://srdata.nist.gov/xps/> (accessed February 23, 2015).
- [58] O.V. Dolomanov, L.J. Bourhis, R.J. Gildea, J.A.K. Howard, H. Puschmann, OLEX²: a complete structure solution, refinement and analysis program, *J. Appl. Crystallogr.* 42 (2009) 339–341, <http://dx.doi.org/10.1107/S0021889808042726>.
- [59] L. Palatinus, G. Chapuis, SUPERFLIP – a computer program for the solution of crystal structures by charge flipping in arbitrary dimensions, *J. Appl. Crystallogr.* 40 (2007) 786–790, <http://dx.doi.org/10.1107/S0021889807029238>.
- [60] G.M. Sheldrick, A short history of SHELX, *Acta Crystallogr. Sect. A* 64 (2008) 112–122, <http://dx.doi.org/10.1107/S0108767307043930>.
- [61] G.M. Badger, *Aromatic Character and Aromaticity*, Cambridge University Press, First Edition edition, 1969.
- [62] M.-Y. Shao, Y.-C. Ho, H.-M. Gau, Reactions of TiCl_4 or $\text{Ti}(\text{O}-i\text{-Pr})\text{Cl}_3$ with 2,4-pentanedione. The molecular structures of $\text{TiCl}_3(\text{acac})(\text{THF})$ and $\text{Ti}(\text{O}-i\text{-Pr})\text{Cl}_2(\text{acac})(\text{THF})$, *J. Mol. Chem. Soc.* 47 (2000) 901–906, <http://dx.doi.org/10.1002/jccs.200000122>.
- [63] V. Nagarajan, B. Müller, O. Storcheva, K. Köhler, A. Pöppel, Coordination of solvent molecules to $\text{VO}(\text{acac})_2$ complexes in solution studied by hyperfine sublevel correlation spectroscopy and pulsed electron nuclear double resonance, *Res. Chem. Intermed.* 33 (2007) 705–724, <http://dx.doi.org/10.1163/156856707782169408>.
- [64] H.J. Kakkonen, J. Pursiainen, T.A. Pakkanen, M. Ahlgrén, E. Iiskola, TiCl_4 diester complexes: relationships between the crystal structures and properties of Ziegler-Natta catalysts, *J. Organomet. Chem.* 453 (1993) 175–184, [http://dx.doi.org/10.1016/0022-328X\(93\)83108-8](http://dx.doi.org/10.1016/0022-328X(93)83108-8).

- [65] P. Sobota, S. Szafert, T. Lis, Reactions of $TiCl_4$ with diesters. Crystal structures of $[CH_2(CO_2Et)2Cl_4Ti]$ and $[C_2H_4(CO_2CH_2CH_2OPh)_2Cl_4Ti]$, *J. Organomet. Chem.* 443 (1993) 85–91, [http://dx.doi.org/10.1016/0022-328X\(93\)80013-2](http://dx.doi.org/10.1016/0022-328X(93)80013-2).
- [66] A.L. Hector, W. Levason, A.J. Middleton, G. Reid, M. Webster, Vanadium(IV) and oxidovanadium(IV) and -(V) complexes with soft thioether coordination – synthesis, spectroscopic and structural studies, *Eur. J. Inorg. Chem.* 2007 (2007) 3655–3662, <http://dx.doi.org/10.1002/ejic.200700349>.
- [67] F. Weinhold, C.R. Landis, *Valency and Bonding: A Natural Bond Orbital Donor-Acceptor Perspective*, Cambridge University Press, Cambridge, UK ; New York, 2005.
- [68] R.F. Barrow, D.A. Long, J. Sheridan (Eds.), *Molecular Spectroscopy*, Vol. volume 5, Royal Society Of Chemistry, 1978.
- [69] P. Sobota, J. Ejfler, S. Szafert, T. Glowiak, I.O. Fritzyk, K. Szczegot, Synthesis and characterization of new di- and tetra-meric vanadium intermediates of olefin polymerization catalysts. Crystal structures of $[V_2(\mu-Cl)2Cl_4(MeCO_2Et)_4]$ and $[(VOCl_2[CH_2(CO_2Et)_2])_4] \cdot 2CH_2Cl_2$, *J. Chem. Soc. Dalton Trans.* (1995) 1727–1732, <http://dx.doi.org/10.1039/DT9950001727>.
- [70] D.C. Crans, R.A. Felty, M.M. Miller, Cyclic vanadium(V) alkoxide. An analog of the ribonuclease inhibitors, *J. Am. Chem. Soc.* 113 (1991) 265–269, <http://dx.doi.org/10.1021/ja00001a038>.
- [71] E.C.E. Rosenthal, From vanadium(V) to vanadium(IV) - and backwards, *Pure Appl. Chem.* 81 (2009) 1197–1204, <http://dx.doi.org/10.1351/PAC-CON-08-08-32>.
- [72] O. Roubeau, Triazole-based one-dimensional spin-crossover coordination polymers, *Chem. Eur. J.* 18 (2012) 15230–15244, <http://dx.doi.org/10.1002/chem.201201647>.
- [73] M. Yuan, E. Wang, Y. Lu, S. Wang, Y. Li, L. Wang, C. Hu, A novel chain-like binuclear vanadium(V) coordination polymer containing mixed ligands: hydrothermal synthesis and crystal structure of $[(VO_2(2,2'-bipy))_2(tp)]_\infty$ ($tp =$ terephthalate), *Inorg. Chim. Acta* 344 (2003) 257–261, [http://dx.doi.org/10.1016/S0020-1693\(02\)01260-4](http://dx.doi.org/10.1016/S0020-1693(02)01260-4).
- [74] C.C. Li, L. Mei, L.B. Chen, Q.h. Li, T.H. Wang, Synthesis of highly aligned and ultralong coordination polymer nanowires and their calcination to porous manganese oxide nanostructures, *J. Mater. Chem.* 22 (2012) 4982–4988, <http://dx.doi.org/10.1039/C2JM15607E>.
- [75] X.-M. Zhang, M.-L. Tong, H.K. Lee, X.-M. Chen, The first noncluster vanadium(IV) coordination polymers: solvothermal syntheses, crystal structure, and ion exchange, *J. Solid State Chem.* 160 (2001) 118–122, <http://dx.doi.org/10.1006/jssc.2001.9202>.
- [76] H. Hosseini-Monfared, N. Asghari-Lalami, A. Pazio, K. Wozniak, C. Janiak, Dinuclear vanadium, copper, manganese and titanium complexes containing *O,O,N*-dichelating ligands: synthesis, crystal structure and catalytic activity, *Inorg. Chim. Acta* 406 (2013) 241–250, <http://dx.doi.org/10.1016/j.ica.2013.04.044>.
- [77] S. Roy, S. Choubey, S. Khan, K. Bhar, J. Ribas, B.K. Ghosh, Synthesis, characterization and magnetic property of a succinate bridged 1D coordination polymer of cobalt(II) containing benzidine as end-capping ligand, *J. Mol. Struct.* 1061 (2014) 54–60, <http://dx.doi.org/10.1016/j.molstruc.2013.12.081>.
- [78] S. Yu, N. Fu, F. Gao, Z. Sui, Synthesis of vanadium nitride by a one step method, *J. Mater. Sci. Technol.* 23 (2007) 43–46.
- [79] A. Ortega, M.A. Roldan, C. Real, Carbothermal synthesis of vanadium nitride: kinetics and mechanism, *In. J. Chem. Kinet.* 38 (2006) 369–375, <http://dx.doi.org/10.1002/kin.20182>.
- [80] D. Marton, K.J. Boyd, A.H. Al-Bayati, S.S. Todorov, J.W. Rabalais, Carbon nitride deposited using energetic species: a two-phase system, *Phys. Rev. Lett.* 73 (1994) 118–121, <http://dx.doi.org/10.1103/PhysRevLett.73.118>.
- [81] N.H. Azhan, K. Okimura, Y. Ohtsubo, S. Kimura, M. Zaghrioui, J. Sakai, Large modification in insulator-metal transition of VO_2 films grown on Al_2O_3 (001) by high energy ion irradiation in biased reactive sputtering, *J. Appl. Phys.* 119 (2016) 55308, <http://dx.doi.org/10.1063/1.4941348>.
- [82] A.M. Nartowski, I.P. Parkin, A.J. Craven, M. MacKenzie, Rapid, solid-state metathesis routes to metal carbides, *Adv. Mater.* 10 (1998) 805–808.
- [83] J.-G. Choi, Ammonia decomposition over vanadium carbide catalysts, *J. Catal.* 182 (1999) 104–116, <http://dx.doi.org/10.1006/jcat.1998.2346>.